EXPONENTIAL TENSORS: A FRAMEWORK FOR EFFICIENT HIGHER-ORDER DT-MRI COMPUTATIONS

Angelos Barmpoutis and Baba C. Vemuri

University of Florida, Gainesville, FL 32611, USA

ABSTRACT

In Diffusion Tensor Magnetic Resonance Image (DT-MRI) processing a 2^{nd} order tensor has been commonly used to approximate the diffusivity function at each lattice point of the 3D volume image. These tensors are symmetric positive definite matrices and the appropriate constraints required in algorithms for processing them makes these algorithms complex and significantly increases their computational complexity. In this paper we present a novel parameterization of the diffusivity function using which the positive definite property of the function is guaranteed without any increase in computation. This parameterization can be used for any order tensor approximations; we present Cartesian tensor approximations of order 2, 4, 6 and 8 respectively, of the diffusivity function all of which retain the positivity property in this parameterization without the need for any explicit enforcement. Furthermore, we present an efficient framework for computing distances and geodesics in the space of the coefficients of our proposed diffusivity function. Distances & geodesics are useful for performing interpolation, computation of statistics etc. on high rank positive definite tensors. We validate our model using simulated and real diffusion weighted MR data from excised, perfusion-fixed rat optic chiasm.

Index Terms— Biomedical imaging, Biomedical image processing, Magnetic resonance imaging, Diffusion processes

1. INTRODUCTION

Data processing and analysis of matrix-valued image data is becoming quite common as imaging sensor technology advances allow for the collection of matrix-valued data sets. In medical imaging, in the last decade, it has become possible to collect magnetic resonance image (MRI) data that measures the apparent diffusivity of water in tissue *in vivo*. A 2^{nd} order tensor has been commonly used to approximate the diffusivity profile at each lattice point of the image lattice [1]. The approximated diffusivity function is given by $\mathbf{g}^T\mathbf{D}\mathbf{g}$, where $\mathbf{g} = [g_1\ g_2\ g_3]^T$ is the gradient unit vector and $\mathbf{D}$ is a 3×3 matrix. This approximation yields a diffusion tensor (DT-MRI) data set $\mathbf{D}_i$, which is a 2D or 3D matrix-valued image, where subscript i denotes location on a 2D or 3D lattice respectively. These tensors $\mathbf{D}_i$ are elements of the space of 3×3 symmetric positive-definite (SPD) matrices.

Mathematically, these SPD tensors belong to a Riemannian symmetric space, where a Riemannian metric, which is affine invariant assigns an inner product to each point of this space. By using this metric, one can perform various computations on the elements of the space [2, 3]. However implementation of algorithms using this affine invariant framework increases significantly the execution time of the algorithms and complex algorithms may not be finish their execution within a reasonable time frame.

Recently, a Log-Euclidean metric was proposed in [4] for computing with tensors. In this work, the elements from the space of SPD tensors, are mapped to a vector space of dimension $\Re^6$ using the matrix logarithm map. Therefore, one can use the Euclidean norm for computations in this space and finally by using the inverse mapping, the data are mapped back to the space of SPD matrices. This framework is quite interesting and has advantages due to its high computational efficiency in comparison to the affine invariant framework.

Both affine invariant and Log-Euclidean frameworks can be employed for processing fields of 2^{nd} order tensors. Use of higher order tensors was proposed in [5] to represent more complex diffusivity profiles which better approximate the diffusivity of the local tissue geometry. However to date, none of the reported methods in literature for the estimation of the coefficients of higher order tensors preserve the positive definiteness of the diffusivity function.

In this paper we propose a novel parameterization of the diffusivity profile that guarantees the positive definite property without the need of any further computation. We present an efficient framework for computing distances and geodesics in the space of the coefficients of our proposed diffusivity function. The key contribution of our work is that we employ this framework for estimating higher (4^{th}, 6^{th} and 8^{nd}) order tensors from diffusion-weighted MR images. Note that we are only interested for symmetric tensors and therefore we consider only even orders. We compare our method with other existing DTI methods showing high efficiency of the proposed method. We present validation of our framework using real diffusion-weighted MR data from excised, perfusion-fixed rat optic chiasm [6].

This research was in part supported by the NIH grants EB004752 and NS42075. Authors thank Drs. T. Shepherd and E. Özarslan for the data.

2. EXPONENTIAL DIFFUSION TENSORS

We define an Exponential Diffusion Tensor (EDT) of **order 2** as a 3×3 symmetric matrix $\mathbf{E}$, which will be used in the following diffusivity function

$$d(\mathbf{g}, \mathbf{E}) = e^{\mathbf{g}^T \mathbf{E} \mathbf{g}} \quad (1)$$

The EDT matrix $\mathbf{E}$ is not necessarily an SPD matrix since the diffusivity function 1 is positive for any symmetric matrix. For example, in the case that $\mathbf{E}$ is the 3×3 zero matrix, we have $d(\mathbf{g}) = e^0 = 1 \; \forall \; \mathbf{g}$. If we use the standard diffusivity function $\mathbf{g}^T \mathbf{D} \mathbf{g}$, the previous example corresponds to the diffusion tensor $\mathbf{D} = \mathbf{I}$. In this case we have $\mathbf{g}^T \mathbf{D} \mathbf{g} = 1 \; \forall \; \mathbf{g}$.

In eq. 1 the diffusivity function was defined by using a 2^{nd} order exponential tensor $\mathbf{E}$. This function $d(\mathbf{g}, \mathbf{E})$ can be generalized by using higher order tensors. In the case of a 4^{th} order symmetric tensor we have 15 unique coefficients collected into a vector $\vec{\mathbf{E}}$ =($E_{4,0,0}$, $E_{0,4,0}$, $E_{0,4,0}$, $E_{2,2,0}$, $E_{0,2,2}$, $E_{2,0,2}$, $E_{2,1,1}$, $E_{1,2,1}$, $E_{1,1,2}$, $E_{3,1,0}$, $E_{3,0,1}$, $E_{1,3,0}$, $E_{0,3,1}$, $E_{1,0,3}$, $E_{0,1,3}$). In the case of higher order tensors we will use the notation E_{p_1,p_2,p_3} to indicate that it is the coefficient of the term ${g_1}^{p_1} {g_2}^{p_2} {g_3}^{p_3}$. By using this notation eq. 1 can be generalized as

$$d(\mathbf{g}, \vec{\mathbf{E}}) = exp\left(\sum_{i=1}^{N} {g_1}^{p_{1i}} {g_2}^{p_{2i}} {g_3}^{p_{3i}} E_{p_{1i},p_{2i},p_{3i}} \right) \quad (2)$$

where in the case of 2^{nd}, 4^{th}, 6^{th} and 8^{th} order $N = 6$, 15, 28 and 45 respectively.

2.1. Distance measure

We can define a distance measure between same order EDTs $\vec{\mathbf{E}}_1$ and $\vec{\mathbf{E}}_2$ by computing the normalized L-2 distance of the corresponding diffusivity functions $d(\mathbf{g}, \vec{\mathbf{E}}_1)$ and $d(\mathbf{g}, \vec{\mathbf{E}}_2)$, given by $dist(\vec{\mathbf{E}}_1, \vec{\mathbf{E}}_2)^2 = \frac{1}{\int d\mathbf{g}} \int \left[d(\mathbf{g}, \vec{\mathbf{E}}_1) - d(\mathbf{g}, \vec{\mathbf{E}}_2) \right]^2 d\mathbf{g}$ where the integration is over the unit sphere (i.e. for all unit vectors $\mathbf{g}$). As an example, the distance between the 2^{nd} order EDT matrices $\mathbf{E}_1 = \mathbf{0}$ and $\mathbf{E}_2 = (\lim_{x \to -\infty} x)\mathbf{I}$ is $dist(\mathbf{E}_1, \mathbf{E}_2)^2 = 1$. This is true, since $d(\mathbf{g}, \mathbf{E}_1) = 1$ and $d(\mathbf{g}, \mathbf{E}_2) = 0 \; \forall \; \mathbf{g}$. However, we need to define a metric that assigns infinite distance between the purely isotropic $d(\mathbf{g}, \mathbf{E}_1)$ and the 'degenerate' case $d(\mathbf{g}, \mathbf{E}_2)$. Here we use the term 'degenerate' in order to highlight the correspondence between $d(\mathbf{g}, \mathbf{E}_2)$ and the standard diffusivity function $\mathbf{g}^T \mathbf{D} \mathbf{g}$, where $\mathbf{D} = \mathbf{0}$. A distance measure that satisfies this property is given by the following equation

$$dist(\vec{\mathbf{E}}_1, \vec{\mathbf{E}}_2)^2 = \frac{1}{4\pi} \int \left[log(d(\mathbf{g}, \vec{\mathbf{E}}_1)) - log(d(\mathbf{g}, \vec{\mathbf{E}}_2)) \right]^2 d\mathbf{g} \quad (3)$$

By analytically computing the integral, eq. 3 can be written in the from of sum of squares, which is very fast to compute. As an example in the case of 2^{nd} order EDTs eq. 3 can be evaluated using 8 additions and 10 multiplications , in the 4^{th} order case using 47 add. and 33 mul.. Due to lack of space we do not provide these formulas, since their derivation is simple.

Note that the metric defined above is rotation invariant in the case of any order exponential tensors. Furthermore, by using this distance measure it is easy to prove that the mean element $\vec{\mathbf{E}}_\mu$ is defined as the Euclidean average $(\vec{\mathbf{E}}_1 + ... + \vec{\mathbf{E}}_N)/N$ (or geometric mean of d_1,...,d_N) and the geodesic (shortest path) between two elements $\vec{\mathbf{E}}_1$ and $\vec{\mathbf{E}}_2$ is defined as Euclidean geodesic $\gamma(t) = (1-t)\vec{\mathbf{E}}_1 + t\vec{\mathbf{E}}_2$, $t \in [0, 1]$.

In the following section we employ this distance measure to define an anisotropy map of $2, 4, 6$ & 8^{th}-order EDTs.

2.2. Distance from the closest isotropic case

In the isotropic case the quantity $d(\mathbf{g}, \vec{\mathbf{E}})$ is the same constant for every unit vector $\mathbf{g}$, forming an isotropic sphere $c = log(d(\mathbf{g})) = c({g_1}^2 + {g_2}^2 + {g_3}^2)^{(K/2)}$, where $c \in \Re$ and K denotes the order of the symmetric tensor $\vec{\mathbf{E}}$ and is even. The above equation is satisfied by: 2^{nd} order exponential diffusion tensors of the form $\mathbf{E} = c\mathbf{I}$, 4^{th} order EDTs of the form $E_{4,0,0} = E_{0,4,0} = E_{0,0,4} = c$, $E_{2,2,0} = E_{0,2,2} = E_{2,0,2} = 2c$, 6^{th} order EDTs of the form $E_{6,0,0} = E_{0,6,0} = E_{0,0,6} = c$, $E_{4,2,0} = E_{4,0,2} = E_{2,4,0} = E_{0,4,2} = E_{2,0,4} = E_{0,2,4} = 3c$, $E_{2,2,2} = 6c$, and 8^{th} order EDTs of the form $E_{8,0,0} = E_{0,8,0} = E_{0,0,8} = c$, $E_{6,2,0} = E_{6,0,2} = E_{2,6,0} = E_{0,6,2} = E_{2,0,6} = E_{0,2,6} = 4c$, $E_{4,4,0} = E_{0,4,4} = E_{4,0,4} = 6c$, $E_{4,2,2} = E_{2,4,2} = E_{2,2,4} = 12c$, where c is a scalar and the rest of the elements of $\vec{\mathbf{E}}$ are equal to zero.

Given an arbitrary K^{th}-order $\vec{\mathbf{E}}$, we can compute the closest isotropy tensor coefficients $\vec{\mathbf{E}}_{iso}$ by finding the scalar c that minimizes the distance of $\vec{\mathbf{E}}$ from the isotropic case. In the 2^{nd}-order case $c = (E_{1,1} + E_{2,2} + E_{3,3})/3$, in the 4^{th}-order case $c = (E_{4,0,0} + E_{0,4,0} + E_{0,0,4} + E_{2,2,0} + E_{0,2,2} + E_{2,0,2})/9$, in the 6^{th}-order case $c = (E_{6,0,0} + E_{0,6,0} + E_{0,0,6} + E_{4,2,0} + E_{4,0,2} + E_{2,4,0} + E_{0,4,2} + E_{2,0,4} + E_{0,2,4} + E_{2,2,2})/27$ and in the 8^{th}-order case $c = (E_{8,0,0} + E_{0,8,0} + E_{0,0,8} + E_{6,2,0} + E_{6,0,2} + E_{2,6,0} + E_{0,6,2} + E_{2,0,6} + E_{0,2,6} + E_{4,4,0} + E_{0,4,4} + E_{4,0,4} + E_{4,2,2} + E_{2,4,2} + E_{2,2,4})/81$.

The function $f_{iso}(\vec{\mathbf{E}}) = dist(\vec{\mathbf{E}}, \vec{\mathbf{E}}_{iso})$ maps the space of $\vec{\mathbf{E}}$ to the space of non-negative real numbers. The smaller the value of the function, the closer is $\vec{\mathbf{E}}$ to the $\vec{\mathbf{E}}_{iso}$. The behavior of the function f_{iso} is similar to that of the well-known fractional anisotropy (FA) map of 2^{nd} order diffusion tensors. To illustrate this, we estimated the DT field and the EDT field from a real dataset, and then we computed the FA and the f_{iso} map respectively (Fig. 1a and 1b). Furthermore, we plot the f_{iso} as a function of FA in Fig.1d. The same figure also contains the plot (in red) of the fitted function $(-c)log(1 - FA)$ for an estimated $c = 0.318$. The inverse of the above function is $1 - exp(-(1/c) f_{iso}(\vec{\mathbf{E}}))$ and can be used to map f_{iso} to values in the interval [0,1] as was done in Fig. 1c.

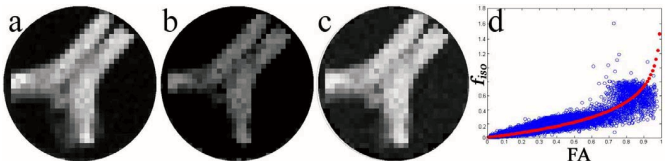

Fig. 1. Comparison between FA and 4^{th}-order f_{iso} map using rat optic chiasm data [6]. a) FA, b) f_{iso}, c) f_{iso} mapped to [0,1] using the fitted function of Fig. 1d, d) plot of f_{iso} vs. FA

2.3. Estimation of EDT field from DWI

The coefficients of any order exponential diffusion tensor can be estimated from diffusion weighted images (DWI) by minimizing the function $E(\vec{\mathbf{E}}, S_0) = \sum_{i=1}^{M}(S_i - S_0 e^{-b_i d(\mathbf{g}_i, \vec{\mathbf{E}})})^2$, where M is the number of diffusion weighted images associated with gradient vectors $\mathbf{g}_i$ and b-values b_i, S_i is the corresponding acquired signal and S_0 is the zero gradient signal. S_0 can either be assumed to be known or estimated simultaneously with the coefficients of $\vec{\mathbf{E}}$. In our experiments we minimized the above equation using simple gradient descent algorithm, however any non-linear functional minimization method can be used. One can use also additional regularization terms in the above function in order to enforce smoothness across the lattice.

2.4. Displacement probability profile

Studies on estimating the fiber orientation from the diffusivity profile has been shown that the peaks of the diffusivity profile does not necessarily yield the orientations of the distinct fiber populations. One should instead employ the displacement probability profiles should [6]. The displacement probability $P(\mathbf{R})$ is given by the Fourier integral $P(\mathbf{R}) = \int E(\mathbf{q}) exp(-2\pi i \mathbf{q} \cdot \mathbf{R}) d\mathbf{q}$ where $\mathbf{q}$ is the reciprocal space vector, $E(\mathbf{q})$ is the signal value associated with vector $\mathbf{q}$ divided by the zero gradient signal and $\mathbf{R}$ is the displacement vector.

In the case of 2^{nd} order exponential diffusion tensors the peak of the diffusivity profile coincides with the peak of the displacement probability profile. Therefore fiber orientation can be estimated as the eigenvector associated with the largest eigenvalue of matrix $\mathbf{E}$. In higher order case, instead of finding the maxima of $P(\mathbf{R})$ we can find the maxima of the expression: $\sum_{i=1}^{N} \int_{-\infty}^{\infty} E(q\mathbf{q}_i)\, exp(-2\pi i q \mathbf{q}_i \cdot \mathbf{R})\, 4\pi q^2\, dq$, which approximates the reciprocal space using the icosahedral tessellation of the unit hemisphere, where q is a scalar and $\mathbf{q}_i$ are unit vectors corresponding to the tessellation. In the case of third-order tessellation we have $N = 81$, which is the approximation that we used in our experiments. By computing the integral analytically in the above approximation we have

$$P(\mathbf{R}) \approx \frac{\sqrt{\pi}}{4N} \sum_{i=1}^{N} exp\left(-\frac{\alpha}{4\beta}\right)\left(\frac{2}{\beta^{5/2}} - \frac{\alpha}{\beta^{3/2}}\right) \quad (4)$$

where $\alpha = (2\pi \mathbf{q}_i \cdot \mathbf{R})^2$, $\beta = 4\pi t d(\mathbf{q}_i, \vec{\mathbf{E}})$ and t is the effective diffusion time.

TABLE A: COMPARISON OF DTI FRAMEWORKS

Frameworks:	Affine invar.	Log-Euc.	EDT framework
Distance map	0.19 sec	0.45 sec	0.04 sec
Smoothing	5.65 sec	0.64 sec	0.10 sec

TABLE B: PROPERTIES OF DTI FRAMEWORKS

Properties / Frameworks	Affine inv.	Log-Euc.	EDT
Affine. Invariance	X		
Rotation Invariance	X	X	X
Fast DTI processing		X	X
Unconstrained estimation			X
Use of higher order tensors			X

3. EXPERIMENTAL RESULTS

In this section we present experimental results using synthetic and real data. All the synthetic data were generated by simulating the MR signal from single fibers or fiber crossings using the realistic diffusion MR simulation model in [7].

In order to compare the time performance of the proposed framework with other existing frameworks (affine invariant [3], and Log-Euclidean [4]) for processing tensor fields we synthesized a single row of a 2^{nd}-order DTI and EDT field of size 10000 and then we applied two simple calculations on every pair of tensors: a)computing their distance and b) smoothing by finding their average using the above mentioned frameworks. According to the times reported in Table A, our framework is the fastest. In the case of smoothing, it is significantly faster than the Affine invariant framework and asymptotically faster than the Log-Euclidean. A comparison of their properties is presented in Table B. Note that only the EDT framework can be used for higher-order approximations.

Furthermore, we estimated the 4^{th}-order exponential tensor field of a dataset acquired from excised, perfusion-fixed rat optic chiasm [6]. Figure 2 shows the displacement probability profiles computed from the estimated field. The probability profiles demonstrate the distinct fiber orientations in the central region of the optic chiasm where myelinated axons from the two optic nerves cross one another to reach their respective contralateral optic tracts. These orientation maps are consistent with other studies on this anatomical region of the rat nervous system [6]. Furthermore the f_{iso} map (Fig. 1c) has slightly brighter intensities in the central region, compared to the FA map (Fig. 1a). This is because FA uses 2^{nd}-order approximation, which fails in approximating the fiber

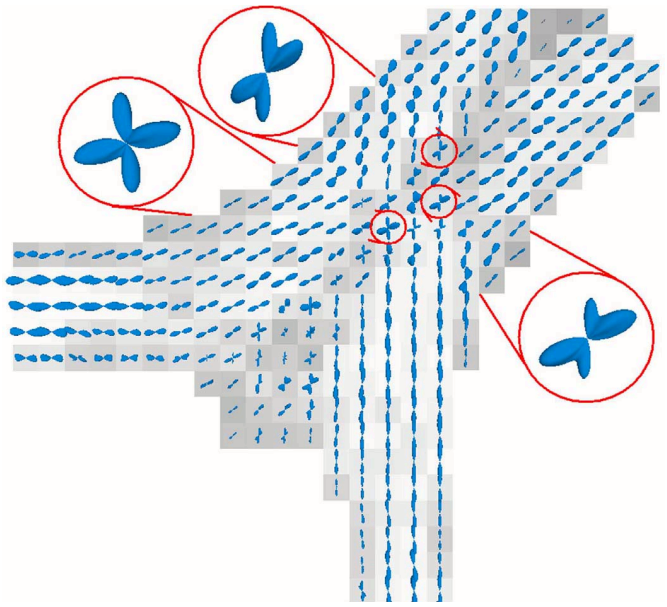

Fig. 2. Displacement probability profiles of a 4^{th}-order EDT field from a rat optic chiasm data set [6]. In the background the distance from the closest isotropy f_{iso} is shown.

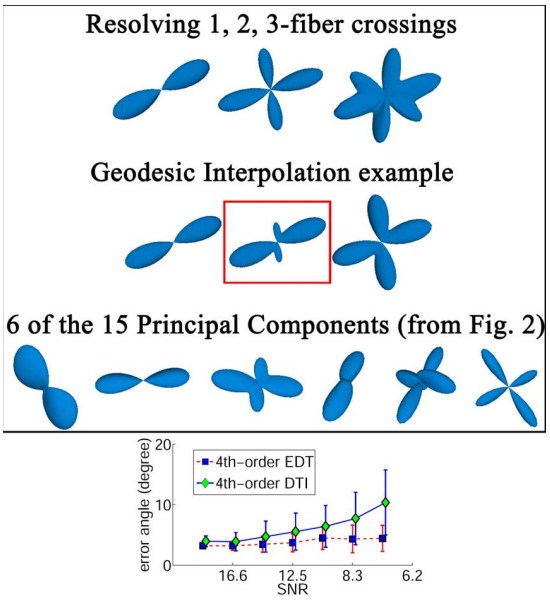

Fig. 3. Top: Uses of the proposed framework for: resolving fiber crossings (8^{th}-order example), geodesic interpolation and calculating PCA (4^{th}-order example) from dataset of Fig. 2. Bottom: Comparison of 4^{th}-order DTI and EDT in estimating fiber orientations for different SNR in the data.

crossings in this region and produces estimations close to the isotropy (darker intensities).

In our framework, after having estimated the coefficient vectors $\vec{\mathbf{E}}$, we can use algorithms developed for vectorfield processing in order to compute statistics (average, principal components), interpolate EDT fields etc. Figure 3 (top) shows some examples of processes for resolving fiber crossings, interpolating and computing principal components using the proposed framework, for the entire image of Fig. 2.

Finally Fig. 3 (bottom) presents a comparison of 4^{th}-order DTI [5] and EDT in estimating fiber orientations using simulated MR signal [7] for different amounts of Riccian noise in the data. The errors observed by using our method are significantly smaller than those of 4^{th}-order DTI, which conclusively validates the accuracy of our proposed method.

4. CONCLUSION

In this paper a novel framework for efficient high-order DT-MRI processing was presented. This framework ensures positive definiteness of the diffusivity profile and can be employed for higher order approximations. A metric was developed for doing computations between same order exponential tensors. The isotropic cases and the distance map from the closest isotropies were also analyzed. Comparisons of the proposed framework with other existing DTI frameworks were presented demonstrating the high efficiency of the proposed method. Finally the proposed framework was validated using simulated and real data from a rat optic chiasm.

5. REFERENCES

[1] P.J. Basser, J. Mattiello, and D. Lebihan, "Estimation of the Effective Self-Diffusion Tensor from the NMR Spin Echo.," *J. Magn. Reson. B*, vol. 103, pp. 247–254, 1994.

[2] P. Fletcher and S. Joshi, "Principal geodesic analysis on symmetric spaces: Statistics of diffusion tensors.," *Proc. of CVAMIA*, pp. 87–98, 2004.

[3] X. Pennec, P. Fillard, and N. Ayache, "A Riemannian framework for tensor computing.," *International Journal of Computer Vision*, vol. 65, 2005.

[4] V. Arsigny, P. Fillard, X. Pennec, and N. Ayache, "Fast and Simple Calculus on Tensors in the Log-Euclidean Framework.," in *Proceedings of MICCAI*, 2005, LNCS, pp. 259–267.

[5] Evren Özarslan, Baba C. Vemuri, and Thomas Mareci, "Fiber orientation mapping using generalized diffusion tensor imaging.," in *ISBI*, 2004, pp. 1036–1038.

[6] Özarslan et al., "Resolution of complex tissue microarchitecture using the diffusion orientation transform (DOT)," *Neuroimage*, vol. 31, no. 3, pp. 1086–103, 2006.

[7] O. Söderman and B. Jönsson, "Restricted diffusion in cylindrical geometry.," *J. Magn. Reson.*, vol. A (117), pp. 94–97, 1995.